Yield strength measurement of ferromagnetic materials based on the inverse magnetostrictive effect

Fei Han[a], Han Yao[b,*], Entao Yao[a], Ping Wang[a], Yu Shi[a] , Yuan Zhang[a]

[a]College of Automation Engineering, Nanjing University of Aeronautics and Astronautics, Nanjing 211106

[b]Department of Physics and Astronomy, University College London, Gower Street, London WC1E 6BT, United Kingdom

* Correspondence: ucapyao@ucl.ac.uk

Abstract: Ferromagnetic materials have been widely used in industry and risk the hazards of aging and degradation of their mechanical properties. This paper proposed a non-destructive method for the measurement of the yield strength of ferromagnetic materials which is influenced by the materials' microstructure. It is based on the fact that the microstructure influences the pattern of the inverse magnetostrictive effect of ferromagnetic materials. To verify the results experimentally, an electromagnetic ultrasonic transducer (EMAT) detection system is set up to measure the yield strength of ferromagnetic materials. We continuously changed the static magnetic field strengths at the receiver of electromagnetic ultrasonic transducer, which caused the inverse magnetostrictive effect change. The relationship between the electromagnetic acoustic transducer signals and the static magnetic field strengths were obtained, from which we extracted the pattern parameters related with the yield strength. The regression model of the pattern parameters versus the yield strength was established and then verified with trials on five test samples. The maximum relative error was 6.3%.

Keywords: inverse magnetostrictive effect, yield strength, electromagnetic ultrasonic transducer, regression model

1 Introduction

The measurement of mechanical properties is fundamental both in industry and scientific research [1,2], and the yield strength is one of the most important mechanical properties. The ferromagnetic materials with the same composition may have different yield strength due to the differences of process conditions. Destructive testing methods [3-5] are costly and thus limited to sampling test. These drawbacks excited the emergence of non-destructive testing (NDT) methods which can achieve real-time monitoring of objects with high accuracy. Owing to the fact that the magnetic properties of ferromagnetic materials, such as permeability and coercivity are relative to the change of their mechanical properties, some non-destructive testing methods (NDT) have been proposed, including the Barkhausen noise method [6], eddy current method, incremental permeability method, etc. [7-8].

Variations in the microstructure of ferromagnetic materials are reflected by changes in magnetic properties. At the same time, material properties change with the variations of microstructure. By the above relationship, it is likely that material properties are related to magnetic properties. To study the relationship between magnetic properties and material properties, Fraunhofer IZFP revealed the correlations between coercivity and the approximate value of skin depth in grinded parts, and this correlations were used to determine the quantitative hardening depth in steel and cast iron components [9-10]. In this way, the magnetic properties are relative to mechanical properties [11]. Later, more magnetic properties, such as remanence and permeability, have been proposed to reflect mechanical properties. Li et al. proposed a multi-feature fusion method dependent on the pulsed eddy current. It is used for testing the yield strength of ferromagnetic materials [12]. This method can measure the yield strength with a maximum relative error of 5.3%, but the eddy current signal is greatly influenced by the lift-off between the probe and the material. Chen et al. proposed that the incremental permeability can be used to detect plastic deformation. However, when this method is used to measure a small change of plastic deformation, its maximum relative error is as high as 20% [13]. Another method based on the Barkhausen noise has been proved useful on the yield strength measurement [14-15], but it can only detect signals on the surface of the material due to the skin effect and is easily disturbed by high frequency noise. Yu et al. proposed a method to monitor the yield strength of the steel strip online [16]. The method periodically magnetizes the steel strip and measured the gradients of the residual magnetic field intensity on the top and bottom of the strips. Its maximum relative error is 10%.

The Electromagnetic Acoustic Transducer (EMAT) is firstly proposed by Thompson [17] and has been applied on defect detections of pipeline and metal plate [18,19]. However, few researches have been reported about applying the EMAT on the yield strength measurements. To explore the application of the EMAT on the yield strength measurements, we set up an experimental platform and an initial study based on the magnetostrictive effect at the transmitter was reported in reference [20] wherein BP neural network was used to establish the relationship between the magnetostrictive characteristic parameters and the yield strength. This model demonstrated the high accuracy with a maximum relative error of 10.36%. Theoretically the magnetostrictive effect and the inverse magnetostrictive effect both influence the EMAT signal. Therefore, further studies based on the inverse magnetostrictive effect are inspired to explore the potentials of more accurate yield strength measurement of the ferromagnetic materials. Since an EMAT does not need couplant, this method has good fidelity for high temperature environment and can be also developed to realize online monitoring of the yield strength.

To study the relationship between the EMAT signal based on the inverse magnetostrictive effect and the yield strength, our experimental platform was further developed. The pattern parameters were extracted from the experimental curves because they were sensitive to the yield strength. As opposed to the BP model in reference [20], we selected regression to build the model between the pattern parameters and the yield strength. The reliability of the model was then proved experimentally.

2 Principle

The ferromagnetic materials with the same composition may have different mechanical properties. Taking the cold-rolled steel plate as an example, due to the differences of processing conditions such as annealing temperature and cold rolling reduction rate, there are also many differences in the sizes of the magnetized domain, grain sizes and orientations of different cold-rolled steel plate, which influence the mechanical and magnetic properties [21]. For example, the annealing temperature changes the grain sizes and their uniformity, which will change the mechanical properties of ferromagnetic materials [22]. Grains are composed of magnetized regions, which is named as magnetic domain. Since the magnetization direction of each magnetic domain is different and averaged out, ferromagnetic materials are not magnetized macroscopically [23]. The external magnetic field applied to the ferromagnetic materials changes the microstructure of the ferromagnetic materials, which causes the permeability to change. This is because the external magnetic field causes the change of grain orientations, resulting in the change of magnetoresistance [24]. Figure1 illustrates the relationship between the magnetization and the permeability curves during the magnetization process [25], where B is the magnetic induction strength of ferromagnetic materials, H is the externally applied magnetic field strength, and $\mu = B/H$ is the permeability of the ferromagnetic materials.

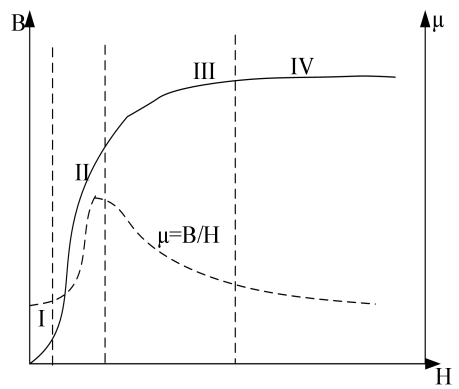

Figure 1. Relationship between the permeability curve and the magnetization curve. The solid line is magnetization curve and the dashed line is permeability curve. The magnetization process can be roughly divided into four stages. Stage I represents the reversible displacement of domain walls. The magnetization curve is linear at this stage. If the external magnetic field is removed,

B decreases to zero. Stage II represents the irreversible displacement of the domain wall. The curve is no longer linear and rises sharply, which is caused by the irreversible jump of the domain wall. At this stage, considerable domains turn to the easy magnetization direction, which is consistent with the direction of external magnetic field. If the external magnetic field strength decreases to zero, the structure of the domain and domain wall cannot return to the initial state. Stage III is about the rotation of domain moment. To be specific, the displacement of domain wall is ended, but with the increase of the external magnetic field strength, the curve still rises slowly and plateaus finally [26].

The mechanical properties of the ferromagnetic materials, such as the yield strength and the tensile strength, are influenced by its microstructure [27]. Owing to the difference of annealing temperature in process conditions, the grain sizes change, which is shown in figure 2. Hall-Petch equation is defined as $\sigma_s = \sigma_0 + kd^{-1/2}$, where σ_s is the yield strength, σ_0 is the lattice friction resistance required to actuate the dislocation, k is a constant related grain boundaries and d is diameter of the grain size. According to Hall-Petch equation, the mechanical properties of ferromagnetic materials are greatly influenced by the grain sizes. When the grain sizes are small, the number of the grain boundaries will increase, which causes the resistance to dislocation glide to increase [28]. The above reasons cause the microstructure to affect the mechanical properties.

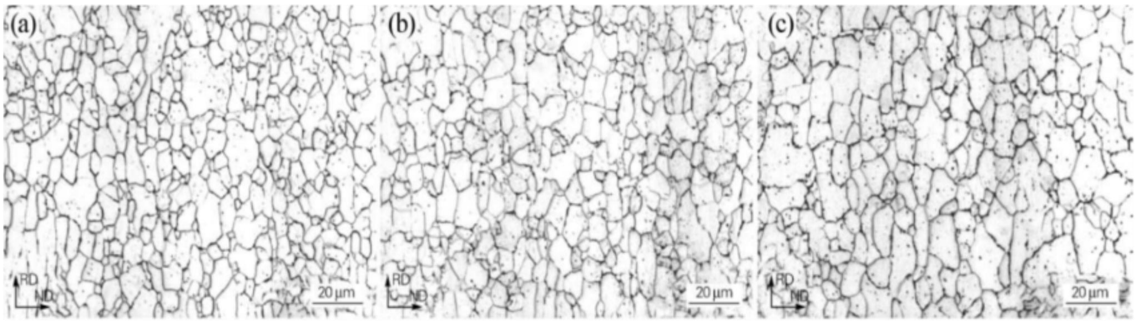

Figure 2. Grain size at different annealing temperatures [22] of (a) 700℃, (b) 740℃ and (c) 780℃. The grain size increases with the annealing temperature.

As discussed before, the magnetic properties, like permeability in figure 1, are also influenced by the microstructure. The mechanical properties and magnetic properties are also influenced by the same microstructure parameters [29]. Therefore, the relationship between the microstructure and the mechanical properties and the relationship between the microstructure and the magnetic properties can be expressed as functions respectively [29]. The yield strength Rp is referred to as a function of the microstructure parameters,

$$Rp = Rp(P_1, P_2, ..., P_n), \tag{1}$$

where P_i is the related microstructure parameters. Likewise, the magnetic properties M_i are also the functions of the microstructure, expressed as

$$M_i = M_i(P_1, P_2, ..., P_n), \tag{2}$$

where i=1, 2, 3…, m. Combining these two equations by eliminating P_i, the relationship between Rp and M_i is

$$Rp = Rp(M_1, M_2, ..., M_m). \tag{3}$$

In this paper, we use EMAT, which excites and receives ultrasonic waves in the ferromagnetic material [30], to measure the magnetic property of the ferromagnetic materials. The magnetostrictive effect and the inverse magnetostrictive effect of the ferromagnetic material are the theoretical basis of an EMAT. When the ferromagnetic materials are subjected to an external magnetic field, the volume and length change slightly, which is named as the magnetostrictive effect. When the materials deform, the permeability will change and subsequently a magnetic field is excited in the materials. The strength of this induced magnetic field varies with the strength of a static magnetic field additionally applied to the material, which is named as the inverse magnetostrictive effect. The conversion mechanism of the transmitter and receiver is shown in figure 3.

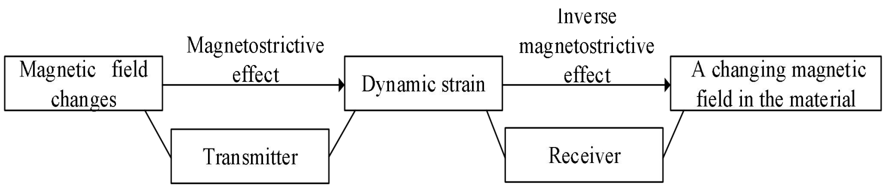

Figure 3. Conversion mechanism of the transmitter and receiver. Due to the magnetostrictive effect at the transmitter, ferromagnetic materials produce dynamic strains, which excites the ultrasonic wave. Then, a changing magnetic field is generated at the receiver by the inverse magnetostrictive effect, which realize the receiving of EMAT signal.

The ultrasonic excitation takes place at the transmitter. An alternating current in the coil can generate eddy currents in the ferromagnetic specimen, which creates a dynamic magnetic field. The specimen will vibrate under the combined effect of the dynamic magnetic field and the static magnetic field provided by the magnet. This vibration causes the ultrasonic wave. The above process can be expressed by the following equations [26],

$$\frac{1}{\vec{\mu}}\nabla^2\vec{A}-\eta\frac{\partial\vec{A}}{\partial t}+\frac{1}{S}\iint_S\eta\frac{\partial\vec{A}}{\partial t}ds=-\frac{\vec{i}}{S}, \tag{4}$$

$$\vec{f}=\vec{f_L}+\overrightarrow{f_{MS}}, \tag{5}$$

$$\vec{f}_L=\overrightarrow{B_0}\times\overrightarrow{J_\omega}, \tag{6}$$

$$\overrightarrow{f_{MS}}=-\nabla_t\left(E^T\vec{H}\right), \tag{7}$$

$$\left(\nabla\cdot\vec{C}\nabla\vec{U}\right)+\vec{f}=\rho\frac{\partial^2\vec{U}}{\partial t^2}, \tag{8}$$

where $\vec{\mu}$ is the magnetic permeability of the test specimen, $\vec{A}$ is the magnetic vector potential, $\vec{i}$ is the total current density in the specimen, η is the conductivity of the specimen, S is the cross-sectional area of the coil. The total force on the material is $\vec{f}$, which is composed of the magnetostrictive force $\overrightarrow{f_{MS}}$ and the Lorentz force $\vec{f_L}$. E^T is the inverse piezomagnetic coefficient matrix, $\vec{C}$ is the stiffness matrix of specimen, ρ is the volume density of material and $\vec{U}$ is the transpose matrix of displacement.

As soon as the ultrasonic wave reaches the receiver, a dynamic magnetic field is generated at the receiver due to the inverse magnetostrictive effect. The coil at the receiver generates the induced voltage in the dynamic magnetic field. This process is described by the following equations [26]

$$\overrightarrow{J_{MS}} = \nabla \times \overrightarrow{B_{MS}(\mu)} , \tag{9}$$

$$\frac{1}{\vec{\mu}}\nabla^2 \vec{A} - \eta \frac{\partial \vec{A}}{\partial t} - \frac{\eta}{S}\frac{\partial}{\partial t}\iint_{\Omega_c} \vec{A} ds = \overrightarrow{J_{MS}} , \tag{10}$$

$$\vec{E} = -\frac{\partial \vec{A}}{\partial t} , \tag{11}$$

$$V = \frac{\int_{\Omega}\int_{l} E \cdot d\vec{l} d\Omega}{\int_{\Omega} d\Omega} , \tag{12}$$

where $\overrightarrow{B_{MS}}$ is the magnetic induction strength of the ferromagnetic material and it is the function of permeability $\vec{\mu}$, $\overrightarrow{J_{MS}}$ is the current density in the specimen at the receiver and V is the induced voltage of the coil at the receiver.

Since we mainly studied the inverse magnetostrictive effect at the receiver of the EMAT, the magnetic field strength at the receiver is adjusted to change the permeability of the materials. As can be seen from equation (13), a change in permeability results in a change in B_{MS} [31]

$$\overrightarrow{B_{MS}} = \mathrm{d}\sigma + \mu_0 \vec{\mu} \vec{H} , \tag{13}$$

where d is the piezomagnetic coefficient, σ is the stress inside the specimen, μ_0 is the free space permeability and its value is $4\pi \times 10^{-7}\,\mathrm{H/m}$, $\vec{H}$ is the static magnetic field strength. According to equation (3), permeability $\vec{\mu}$ can be used to represent the yield strength. Likewise, equation (13) reflects that $\vec{\mu}$ changes $\overrightarrow{B_{MS}}$, which accordingly changes the amplitude of EMAT signal depends on equations (9)-(12). Therefore, the EMAT signal can be used to reflect the yield strength of ferromagnetic materials.

3 EMAT detection system

Generally speaking, the EMAT detection system is divided into three modules, an electromagnetic ultrasonic transmitting circuit, an electromagnetic ultrasonic transducer and an electromagnetic ultrasonic receiving circuit. When the EMAT detection system works, the pulse transmitting circuit with a single chip microcomputer as the core transmits the high-frequency pulse train (200KHz in the experiment). After the power amplifier circuit and the impedance matching network, the pulse train is fed to the coil. Under the effect of the DC electromagnet, the transmitting coil can excite a series of vibration signals of the same frequency on the surface of the tested specimen, namely the ultrasonic wave. When the ultrasonic wave is transmitted to the coil at the receiver, the coil generates an induced voltage with a small amplitude. After the filtering and amplifying circuit, the electric signal can be directly collected by the data acquisition card to the PC for processing [32,33]. The electromagnetic ultrasonic detection system is shown in figure 4.

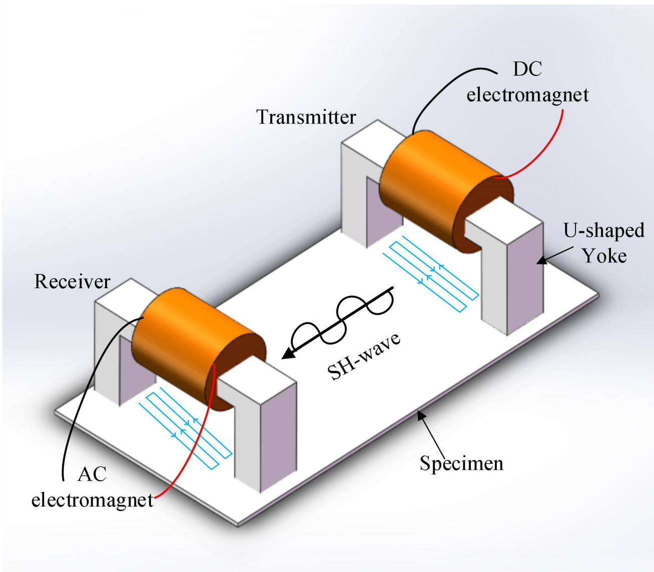

Figure 4. Schematics of the EMAT detection system. An EMAT consists of U-shaped magnet and meander-line coil. A DC electromagnet is used to provide a constant static magnetic field at the transmitter. An AC electromagnet is used to change the static magnetic field strength at the receiver. A meander-line coil (not shown in the figure) is placed on the surface of the

ferromagnetic specimen to excite a single direction SH-wave. According to the Faraday's law, an eddy current, opposite to the direction of the current in the coil, is generated in the specimen. The directions of the static magnetic field and the dynamic magnetic field generated by the induced eddy current are perpendicular to each other.

The excitation and reception of the ultrasonic wave in the ferromagnetic materials can be realized either by a Lorentz force or a magnetostrictive force [34]. As the effect of the inverse magnetostriction on the electromagnetic ultrasonic transducer is studied in this paper, the meander-line coil and the magnet are positioned to avoid the influence of the Lorentz force, as is shown in figure 5. In figure 5, since the direction of the bias magnetic field is parallel to the direction of the eddy current generated by the coil in the testing sample, so the influence of the Lorentz force can be ignored [26].

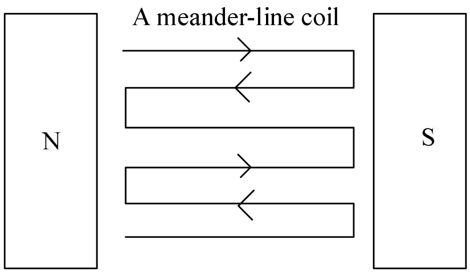

Figure 5. Relationship between the magnet and the coil. The direction of the current in the coil is parallel to that of the external magnetic field, thus avoiding the influence of the Lorentz force as much as possible.

The static magnetic field at the transmitter is provided by a DC electromagnet and the direction of this field is parallel to the direction of the current in the long side of the meander-line coil. Under the cooperation of the static magnetic field and the induced dynamic magnetic field, the ferromagnetic specimen generates periodic deformation which is in phase with the dynamic magnetic field, thus the SH-wave is excited inside the specimen. When the SH-wave signal reaches the receiver, the meander-line coil picks up an induced voltage, which is the EMAT signal. The static magnetic field strength at the receiver is adjusted by an AC electromagnet to change the permeability of the material and then the amplitude of EMAT signal.

4 Experiments and analysis

In this paper, five cold-rolled strip steel specimens of the same length and width, 200 mm × 300 mm, were used. Table 1 shows their thickness, nominal yield strengths and initial permeability.

Table 1 Parameters of specimens

Specimen	1	2	3	4	5
Thickness/mm	0.66	0.75	0.65	0.70	0.75
Yield strength/MPa	144	162	248	283	363
Initial permeability/H/ m	0.052	0.051	0.052	0.051	0.051

In the experiment, the static magnetic field strength at the transmitter remained fixed, and that at the receiver was changed by adjusting the AC electromagnet. Since the energy will decay in the process of ultrasonic transmission, the amplitude of EMAT signal is related to the ultrasonic transmission distance (the distance between the transmitter coil and the receiving coil), and with the increase of the distance, the EMAT signal amplitude gradually decreases. Owing to this reason, we set the distance between the receiving coil and the transmitting coil as 20cm. The corresponding electromagnetic ultrasonic waves were recorded for the five specimens respectively, and we selected one of them to show in figure 6. It can be seen from figure 6 that we chose the current intervals between the two peaks I_p, the current intervals between two valleys I_v, the peak-to-valley value E_p, the slope k (between the right peak and two amperes) and the area of the curve S as a set of pattern parameters.

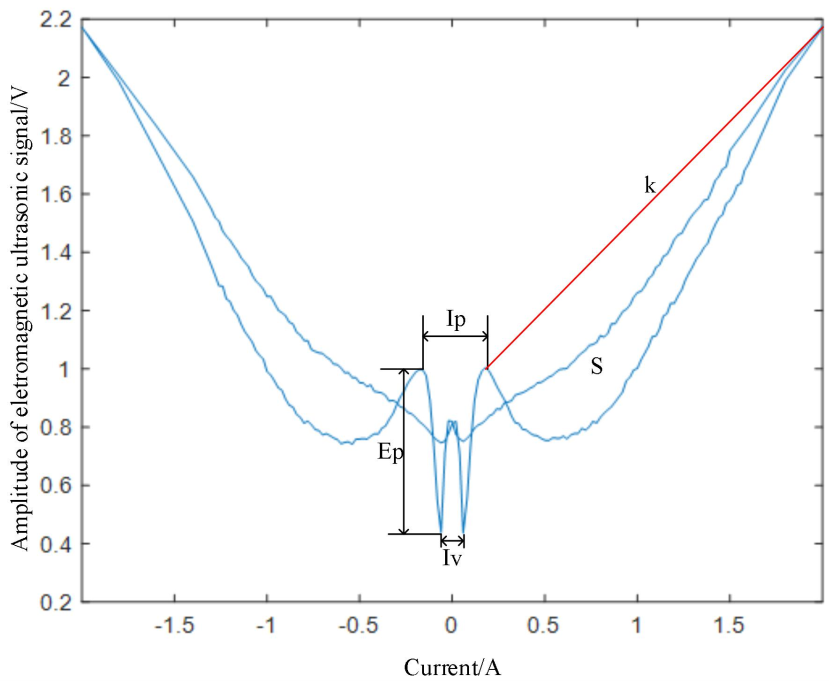

Figure 6. Relationship between the amplitude of EMAT and the current at the receiver; The slope k is calculated between the points of right peak and two amperes. The amplitude of EMAT signal is the induced voltage V in equation (12) and the value of current can represent the static magnetic field strength at the receiver. A W-shaped curve has two local peaks and two local valleys between the two linear zones. In this stage, the permeability mainly affects the amplitude of the EMAT signal. In the linear parts the EMAT signal is dominated by the static magnetic field.

Five measurements were performed for each specimen. The experimental data were shown in figure 7. Figure 7 suggest that Iv, Ip and Ep increase approximately with the increase of the yield strength. On the contrary, S and k decrease with the increase of the yield strength. At the same time, we also used Pearson correlation coefficient to analyze the relationship between pattern parameters and the yield strength, which is shown in Table 2. Table 2 suggests a strong correlation between the pattern parameters and the yield strength of specimens, which is consistent with the variation trend of pattern parameters in figure 7. To predict of the yield strength of each specimen, multiple linear regression analysis was applied to the 20 experimental results by Statistical Product and Service Solutions (SPSS). The values of R^2 and the adjusted R^2 of the obtained linear model was only 0.976 and 0.972, indicating that the linear regression model was reliable. The final regression equation of the yield strength y was given as

$$y=175.8+35.37*I_v+227.5*\Delta I_p-42*S+23.1*k+91.5*E_p \tag{14}$$

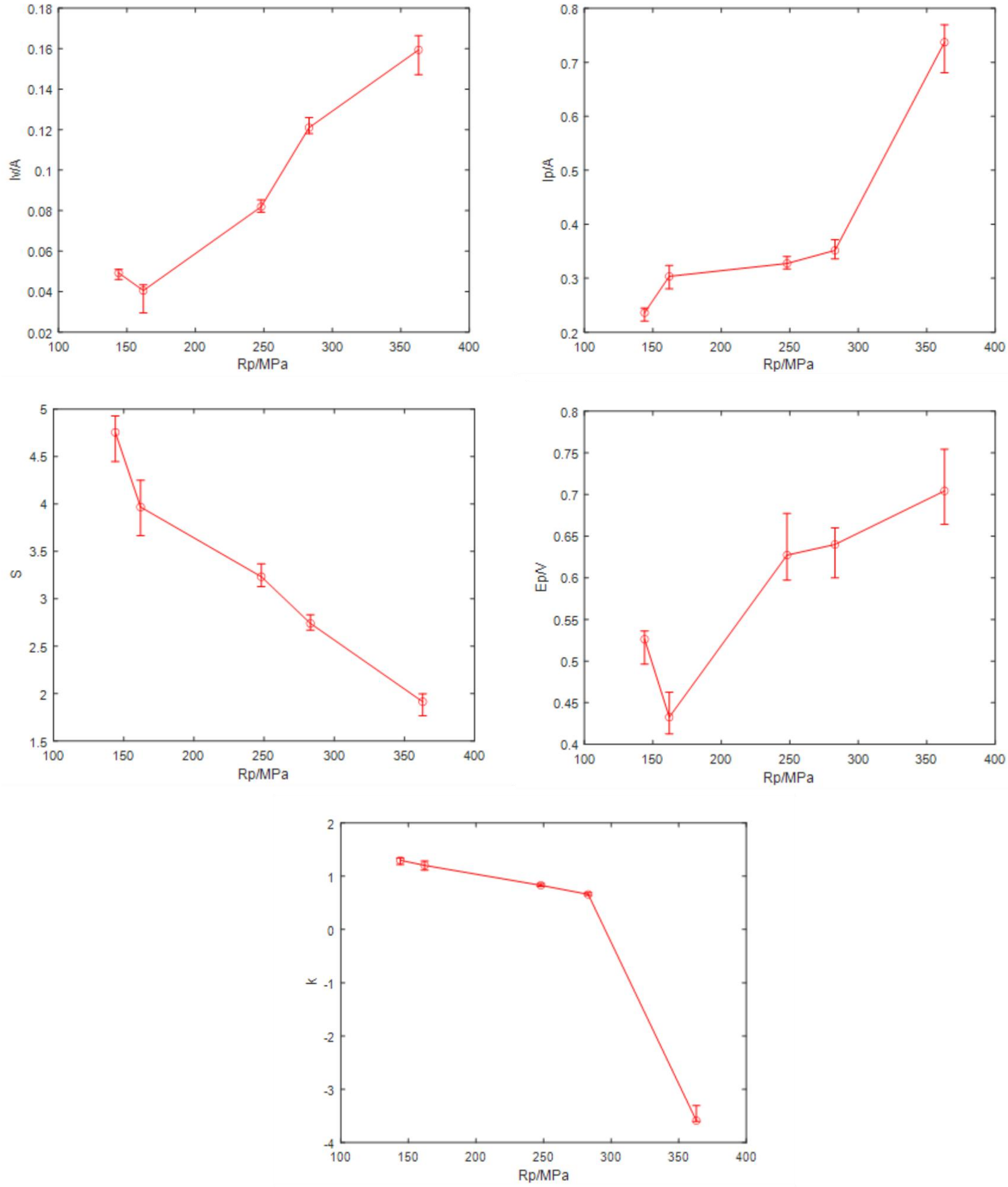

Figure 7. Relationships between yield strength and the pattern parameters. Each pattern parameter has an approximate linear relation with the yield strength. The current intervals between the two peaks I_p, the current intervals between two valleys I_v and

the peak-to-valley value E_p increase with the yield strength Rp, while the slope k and the area of the curve S decrease with the increase of the yield strength Rp.

Table 2 Pearson correlation coefficient between pattern parameters and the yield strength Rp

Pattern parameters	Iv	Ip	S	k	Ep
Rp	0.98	0.86	-0.97	-0.84	0.91

In order to verify the reliability of the regression model, we used the established model to test the remaining five samples and used the relative error to evaluate the accuracy of the model. Relative error is defined as

$$RE = \left| \frac{y_i^{'} - y_i}{y_i} \right| \times 100\% , \quad (15)$$

where $y_i^{'}$ is the predicted value and y_i is the actual value. Figure 8 shows the prediction results of the remaining samples obtained by the regression equation. The maximum relative error is 6.3%. Therefore, the regression model is considered qualified for the yield strength measurement.

The thickness of the specimens in this paper ranges from 0.65mm to 0.75mm. Compared with the model in reference [17], when the model presented in this paper is used to test a thicker specimen, the amplitude of EAMT signal will drown in the noise and cannot be analyzed effectively. Besides, we do not have enough samples of the similar thickness. Both of these could cause the prediction error.

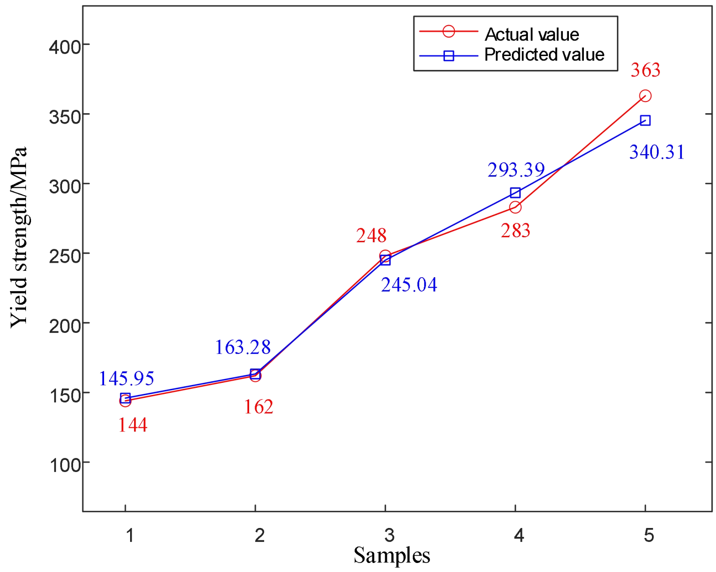

Figure 8. Comparison between predicted values(bule) and actual values(red). The relative error is between 0.1% and 6.3%, which verifies the accuracy of this model.

5 Conclusion

In this paper, a method based on the inverse magnetostrictive effect of EMAT was proposed to realize the non-destructive testing measurement of the yield strengths of ferromagnetic materials. The yield strength can be indicated by the curve of the applied static magnetic field and the amplitude of the EMAT signal. A regression model was developed to describe the yield strength as a function of the pattern parameters extracted from the curves. Testing samples showed a maximum relative error of 6.3%, proving the feasibility of our method to measure the yield strength of the cold rolled steel with the same composition and different process conditions. Accuracy can be further improved by adding a filtering function or increasing the number of samples in subsequent studies.

Acknowledgement

We are supported by the special program for Key Scientific Instrument and Equipment Development of the Ministry of Science and Technology (No.2016YFF0103702), the National Natural Science Foundation of China (NO.62073162), and the Key Laboratory of Non-destructive testing and monitoring technology for high-speed transport facilities of the Ministry of Industry and Information Technology.

References

[1]X M Liu, 'The present situation and direction of physical properties testing technology of metal materials (in Chinese)', China Metal Bulletin, No 12, pp 240+242, December 2018. Doi: 10.3969/j.issn.1672-1667.2018.12.148

[2] E G Xiong, 'A theoretical research on magnetic nondestructive testing of steel structures', China Sciencepaper, No 7, pp 492-496, July 2008. DOI: 10.3969/j.issn.2095-2783.2008.07.004

[3] W L Yu, 'Study of the latest development and trend of hardness measurement technology', Physical Testing and Chemical Analysis(Part A:Physical Testing), No 8, pp 401-405, August 2003.Doi:10.3969/j.issn.1001-4012.2003.08.005

[4] H B Huang and F Li, 'Study on mechanical properties of composite materials by in-situ tensile test', Journal of Southeast University (English Edition), No 1, pp 49-52, March 2004. Doi:10.3969/j.issn.1003-7985.2004.01.010

[5] Y P Shi, X P He, Y Q Wang, Y Luo and G Shi, 'Test studies on fatigue performance of aluminum alloys used in construction', Journal of Tsinghua University(Science and Technology), Vol 49, No 9, pp 1437-1440, September 2009.Doi:10.3321/j.issn:1000-0054.2009.09.003

[6] H Barkhausen, 'Two phenomena revealed with the help of new amplifiers', Phys, Vol 20, pp 1-3, January 1919.

[7]X J Wu, Q Zhang and G T Shen, 'Review on advances in pulsed eddy current nondestructive testing technology', Chinese Journal of Scientific Instrument, Vol 37, No 8, pp 1698-1712, August 2016.DOI：10.19650/j.cnki.cjsi.2016.08.003

[8] L J Li, S J Xie, H E Chen and et al., 'Influence of Plastic Deformation on Signals of Magnetic Incremental Permeability for Carbon Steel', China Mechanical Engineering, Vol 29, No 14, pp 1653-1660, July 2018. Doi:10.3969/j.issn.1004-132X.2018.14.003

[9] P Höller, 'Nondestructive Analysis of Structure and Stresses by Ultrasonic and Micromagnetic Methods', Springer US, pp 211-212, 1987. ISBN:78-1-4684-5340-9

[10] I Altpeter, G Dobmann and W A Theiner, 'Quantitative hardening-depth-measurements up to 4 mm by means of micromagnetic microstructure multiparameter analysis-3MA', Rev. Prog. Quant. Nondestruct. Eval, pp 1471-1475, 1987.

[11] B Wolter, Y Gabi and C Conrad, 'Nondestructive Testing with 3MA—An Overview of Principles and Applications', Applied sciences, Vol 9, No 6, March 2019. DOI:10.3390/app9061068

[12] K Y Li, W J Gao, P Wang, Y Y Zhang and C Hang, 'Yield Strength Testing Method of Ferromagnetic Materials Based on Pulsed Eddy Current', China Mechanical Engineering, Vol 30, No 18, pp 2143-2149, September 2019.DOI:10.1088/1757-899X/452/2/022070

[13] H E Chen, S J Xie, Z M Chen and et al., 'Quantitative Nondestructive Evaluation of Plastic Deformation in Carbon Steel Based on Electromagnetic Methods', Materials Transactions, Vol 55, No 12, pp 1806-1815, December 2014.DOI:10.2320/matertrans.M2014173

[14] Y Zhang, 'Non-destructive Testing of High Strength Steel Based on Magnetic Barkhausen Noise', Master's thesis in Huazhong University of science and technologys, May 2015.

[15] S Y Gu, 'Investigation of ferromagnetic materials' mechanical properties based on magnetic barkhausen noise detection', Master's thesis in Nanjing University of Aeronautics and Astronautics, March 2018.

[16]H Y Yu, H S Yu and Y J Guo, 'The introduction and application of EMG on-line testing system for

mechanical properties of strip steel(in Chinese)', Metallurgical Industry Automation,2020, Vol 44, No S1, pp 246-250, August 2020. DOI: CNKI:SUN:YJZH.0.2020-S1-065

[17] R B Thompson, 'A Model for the Electromagnetic Generation and Detection of Rayleigh and Lamb Waves', Sonics and Ultrasonics, IEEE Transactions on, Vol 20, No 4, pp 340-346, 1973.DOI: 10.1109/T-SU.1973.29770

[18] S L Huang, Z Wang, S Wang and W Zhao, 'Review on advances of pipe electromagnetic ultrasonic guided waves technology and its application', Chinese Journal of Scientific Instrument, Vol 39, No 3, pp 1-12, March 2018. DOI:10.19650/j.cnki.cjsi.J1702867

[19] L J Yang, Y H Xing, J Zhang and S W Gao, 'Crack defect detection of aluminum plate based on electromagnetic ultrasonic guided wave', Chinese journal of scientific instrument, Vol 39, No 4, pp 150-160, April 2018.DOI：10.19650/j.cnki.cjsi.J1702976

[20] P Wang, Y Zhang, E T Yao and et al, 'Method of measuring the mechanical properties of ferromagnetic materials based on magnetostrictive EMAT characteristic parameters', Measurement, Vol 168, article number 108187, January 2021. DOI:10.1016/j.measurement.2020.108187

[21]X Song, G J Wang, H P Zheng and T Q Chen, 'Effect of different processes on mechanical properties and yield ratio of low carbon steel plate', Steel Rolling, Vol 31, No 3, pp 9-12+17, June 2014. DOI:

10.3969/j.issn.1003-9996.2014.03.003

[22] X Tang, T F Li, T T Li and H L Li, 'Influence factors on properties of SPCC cold rolled sheet after continuous annealing', Heat treatment of metals, Vol 38, No 9, pp 60- 64, September 2013. DOI:10.13251/j.issn.0254-6051.2013.09.017

[23] BD Cullity and CD Graham 1972 Introduction to Magnetic Materials (London: Addison-Wesley)

DOI：10.1016/S1369-7021(09)70091-4

[24] K Yang, 'Effects of cold-rolling and annealing technologies on microstructure and property of cold rolled non-oriented silicon steel', Master's thesis in Hebei Polytechnic University, March 2009.

[25] G Dobmann, 'Non-destructive testing for ageing management of nuclear power components', Nuclear power-control, reliability and human factors, Vol 34, No 17, pp 311-338, 2011.DOI: 10.5772/17581

[26] S L Huang, S Wang and W Zhao, 'Theory and application of electromagnetic ultrasonic guided wave', Tsinghua university press, pp 2+74-76, October 2013.DOI:10.1007/978-981-13-8602-2

[27] H Jin, Z H Nie, Y L Lian, L Wang and et al, 'Development of Fe 100- x (NiCoMn) x magnetostrictive alloys with good mechanical properties', Journal of alloys and compounds, Vol 810, article number 151931, November 2019. DOI:10.1016/j.jallcom.2019.151931

[28] G X Hu, 'Fundamentals of materials science', Shanghai Jiao Tong University Press, 2001. ISBN：7-313-02480-0

[29] I Altpeter, R Becker, G Dobmann and et al, 'Robust solutions of inverse problems in electromagnetic non-destructive evaluation', Inverse problems, Vol 18, No 6, pp 1907-1921, November 2002.Doi:10.1088/0266-5611/18/6/328

[30] X C Song, Z S Jin and Hao Yu, 'Influences of magnetic circuit structure of magnetostrictive guided wave transducer on the homogeneity of bias magnetic field', International journal of applied electromagnetics and mechanics, Vol 33, No 1, pp 581-588, October 2010. Doi:10.3233/JAE-2010-1161

[31] W P Ren, 'Research and application of EMAT's conversion mechanism in steel plate', Doctoral thesis in university of science and technology Beijing, 2019.

[32] P Li, S L Huang and K Wang, 'Development of a Pulse Exciting Source for Electromagnetic Ultrasonic Detection', Electrical Measurement & Instrumentation, Vol 49, No 2, pp 76-79, February 2012. Doi: 10.3969/j.issn.1001-1390.2012.02.018

[33] X P Liu, 'Investigation on Power MOSFFT′s Gate Driving Circuit', Electrical Switch, Vol 40, No 2, pp 1-2, April 2002. Doi:10.3969/j.issn.1004-289X.2002.02.001

[34] R Ribichini, P B Nagy, and H Ogi, 'The impact of magnetostriction on the transduction of normal bias field EMATs', Ndt& E International, Vol 51, pp 8-15, October 2012. DOI: 10.1016/j.ndteint.2012.06.004

Biographic Footnote

Entao Yao received the Ph.D. degree from Nanjing University of Aeronautics and Astronautics in 1999 and was appointed as professor in 2007. His major is NDT and measurement.

Fei Han received the B.E. degree in measurement and instrumentation from Nanjing Information Engineering University, Nanjing, China, in 2019. His current research interest is Electro-magnetic NDT.

Han Yao is in Department of Physics and Astronomy, University College London, Gower Street, London WC1E 6BT, United Kingdom

Ping Wang received the Ph.D. degree from Southeast University in 2004 and was appointed as professor in 2016. His major is NDT and measurement.

Yu Shi received the Ph.D. degree from Nanjing University of Aeronautics and Astronautics in 2002 and is appointed as teacher in Nanjing University of Aeronautics and Astronautics. Her major is NDT and measurement.

Yuan Zhang received the B.E. degree in measurement and instrumentation from Beijing University of Aeronautics and Astronautics, Beijing, China, in 2019. Her current research interest is Electro-magnetic NDT.